

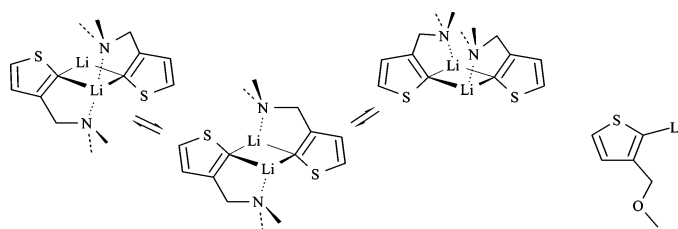
## Solution Structure and Chelation Properties of 2-Thienyllithium Reagents

Kevin L. Jantzi,<sup>†</sup> Craig L. Puckett, Ilia A. Guzei, and Hans J. Reich\*

Department of Chemistry, University of Wisconsin, 1101 University Avenue, Madison, Wisconsin 53706

reich@chem.wisc.edu

Received March 23, 2005



The solution and chelation properties of 2-thienyllithium reagents with potential amine and ether chelating groups in the 3-position and related model systems have been investigated using low temperature <sup>6</sup>Li, <sup>7</sup>Li, <sup>13</sup>C, and <sup>31</sup>P NMR spectroscopy, <sup>15</sup>N-labeling, and the effect of solvent additives. In THF–ether mixtures at low temperature 3-(*N,N*-dimethylaminomethyl)-2-thienyllithium (**4**) is ca. 99% dimer (which is chelated) and 1% monomer (unchelated), whereas 3-(methoxymethyl)-2-thienyllithium (**5**) is <10% dimer. Compound **5** crystallizes as a THF-solvated dimer, but there is no indication that the ether side chain is chelated in solution. Both **4** and **5** form PMDTA-complexed monomers almost stoichiometrically, similar to the model compound **2**, in sharp contrast to phenyl analogues, which show very different behavior. The barriers to dimer interconversion are ca. 2 kcal/mol lower and chelation is significantly weaker in the 2-thienyllithium reagents than in their phenyl analogues.

Many types of aryllithium reagents and organometallic reagents derived from them (such as organocuprates) have found extensive use in synthetic practice for the introduction of carbocyclic and heterocyclic substituents.<sup>1</sup> Many of these reagents have potential chelating groups at *ortho* positions, which serve both to facilitate preparation of the lithium reagent by metalation<sup>2</sup> and to carry additional functionality into the synthetic target. A detailed understanding of the effects of structural changes in the aryllithium on the reactivity and selectivity of its reactions requires knowledge of the solution structure of the reagents involved.

We have recently reported on the solution structures and chelation properties of a series of 2-substituted phenyllithium compounds with pendant ether and amine side chains (**6**–**12**).<sup>3a–d</sup> It was found that both five ring

amines and ethers (**6** and **8**) are strongly chelated and that the chelation strength decreases as the side chain

(3) (a) Reich, H. J.; Gudmundsson, B. Ö. *J. Am. Chem. Soc.* **1996**, *118*, 6074–6075. (b) Reich, H. J.; Goldenberg, W. S.; Sanders, A. W.; Tzschucke, C. C. *Org. Lett.* **2001**, *3*, 33–36. (c) Reich, H. J.; Goldenberg, W. S.; Sanders, A. W.; Jantzi, K. L.; Tzschucke, C. C. *J. Am. Chem. Soc.* **2003**, *125*, 3509–3521. (d) Reich, H. J.; Goldenberg, W. S.; Gudmundsson, B. Ö.; Sanders, A. W.; Kulicke, K. J.; Simon, K.; Guzei, I. A. *J. Am. Chem. Soc.* **2001**, *123*, 8067–8079. (e) X-ray crystal structure of 5-methyl-2-thienyllithium tetramer: Powell, D. R.; Whipple, W. L.; Reich, H. J.; Whipple, W. L. *Can. J. Chem.* **2005**, in press. (f) Reich, H. J.; Green, D. P.; Medina, M. A.; Goldenberg, W. S.; Gudmundsson, B. Ö.; Dykstra, R. R.; Phillips, N. H. *J. Am. Chem. Soc.* **1998**, *120*, 7201–7210. (g) Reich, H. J.; Goldenberg, W. S.; Sanders, A. W. *ARCHIVOC* **2004** (xiii) 97–129 ([http://www.arkat-usa.org/ark/journal/2004/113\\_Krohn/1230/KK-1230F.asp](http://www.arkat-usa.org/ark/journal/2004/113_Krohn/1230/KK-1230F.asp)). (h) Reich, H. J.; Green, D. P. *J. Am. Chem. Soc.* **1989**, *111*, 8729–8731. Reich, H. J.; Borst, J. P.; Dykstra, R. R.; Green, D. P. *J. Am. Chem. Soc.* **1993**, *115*, 8728–8741. Sikorski, W. H.; Reich, H. J. *J. Am. Chem. Soc.* **2001**, *123*, 6527–6535. (i) Reich, H. J.; Sikorski, W. H.; Gudmundsson, B. Ö.; Dykstra, R. R. *J. Am. Chem. Soc.* **1998**, *120*, 4035–4036. (j) Temperatures in the NMR sample were measured using a small amount of 10% <sup>13</sup>C-enriched (Me<sub>3</sub>Si)<sub>3</sub>CH. The chemical shift between the methyne and methyl carbons is strongly (and almost linearly) dependent on temperature. Sikorski, W. H.; Sanders, A. W.; Reich, H. J. *Magn. Reson. Chem.* **1998**, *36*, S118–S124. (k) DNMR simulations and integrations of overlapping peaks were performed with a version of the computer program WINDNMR (Reich, H. J. *J. Chem. Educ. Software* **1996**, 3D, 2; <http://www.chem.wisc.edu/areas/reich/plt/wind-nmr.htm>).

\* To whom correspondence should be addressed.

<sup>†</sup> Current address: Valparaiso University, Valparaiso, IN 46383.

(1) Gilman, H.; Morton, J. W., Jr. *Org. React.* **1954**, *8*, 258–304. Gschwend, H. W.; Roderiguez, H. R. *Org. React.* **1979**, *26*, 1–360. Clark, R. D.; Jahangir, A. *Org. React.* **1995**, *47*, 1.

(2) Klein, K. P.; Hauser, C. R. *J. Org. Chem.* **1967**, *32*, 1479–1483. Snieckus, V. *Chem. Rev.* **1990**, *90*, 879–933. Beak, P.; Snieckus, V. *Acc. Chem. Res.* **1982**, *15*, 306–312. Clayden, J. *Organolithiums: Selectivity for Synthesis*; Pergamon Press: New York, 2002; p 28f.

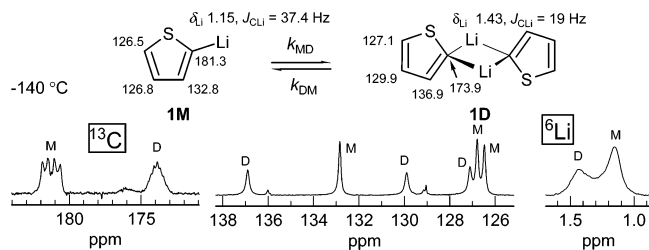
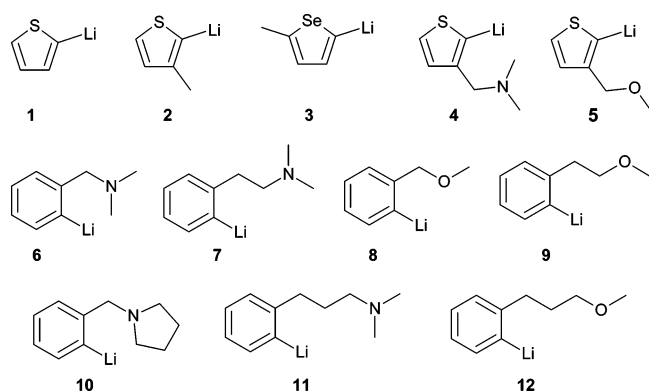


**FIGURE 1.**  $^{13}\text{C}$  and  $^6\text{Li}$  spectra of 0.3 M **1** in 3:2:1 THF/Me<sub>2</sub>O/Et<sub>2</sub>O (D = dimer, M = monomer) at  $-140\text{ }^\circ\text{C}$ .

is lengthened. As a followup to these studies we now report a NMR spectroscopic investigation of some related compounds in the 2-lithiothiophene series to establish the solution structure of model systems (**1** and **2**) and determine the effect of chelation on aggregation state (**4** and **5**). One specific aim was to establish whether there was any generality to the interesting but poorly understood empirical observation that those 2-substituted phenyllithium reagents that were chelated were also significantly more strongly dimerized than nonchelated models. To our knowledge, the solution properties of the easily prepared and synthetically useful thienyllithiums have not been reported, although several single-crystal X-ray structures have been published<sup>3e,4a</sup> and others have been deposited in the Cambridge Structural Database.<sup>4b,c</sup>



## Results and Discussion

**2-Thienyllithium (1).** The  $^{13}\text{C}$  NMR spectrum of **1** in 3:2:1 THF/Me<sub>2</sub>O/Et<sub>2</sub>O<sup>5,6</sup> at  $-140\text{ }^\circ\text{C}$  shows two sets of peaks in a 2:1 ratio (Figure 1, Table S-8<sup>7</sup>). Most diagnostic are the  $^7\text{Li}$ -coupled carbanion signals at  $\delta$  181.2 and 173.9, the former a 1:1:1:1 quartet ( $^7\text{Li}$   $I = 3/2$ ) with  $^1J_{^{13}\text{C}-^7\text{Li}} = 37.4\text{ Hz}$ . This pattern is characteristic of

(4) (a) Benzothiothiophene-TMEDA dimer: Harder, S.; Boersma, J.; Brandsma, L.; Kanters, J. A.; Bauer, W.; Pi, R.; Schleyer, P. v. R.; Schöllhorn, H.; Thewalt, U. *Organometallics* **1989**, *8*, 1688–1696. (b) The single-crystal X-ray structure of the A-type TMEDA-complexed dimer of **4** is reported in the Cambridge Structural Database as private communication: Spek, A. L.; Lakin, M. T.; den Besten, R. (LEDSSES). (c) Other lithiothiophene structure in the Cambridge Structural Database as private communications. 3-Methoxy-2-lithiothiophene: Spek, A. L.; Veldman, N. (HIGPOC); 3-bromo-2-lithiothiophene-TMEDA dimer: Spek, A. L. (HIGXUQ); 2-lithiothiophene dimer: Spek, A. L.; Smeets, W. J. J. (JUJXER).

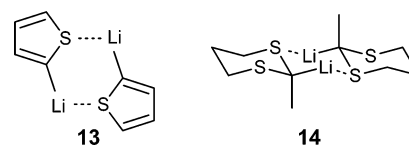
(5) We have used two solvent systems, 3:2 THF/ether (usable to  $-135\text{ }^\circ\text{C}$ ) and 3:2:1 THF/Me<sub>2</sub>O/Et<sub>2</sub>O (required for temperatures below  $-135\text{ }^\circ\text{C}$ ). Both have similar solvent strength, at least as judged by monomer–dimer ratios of 2-ethylphenyllithium.<sup>3c</sup>

(6) Fraser, R. R.; Mansour, T. S.; Savard, S. *Can. J. Chem.* **1985**, *63*, 3505.

(7) See Supporting Information.

monomeric organolithium reagents. The signal at  $\delta$  173.9 is a poorly resolved heptet with  $^1J_{^{13}\text{C}-^7\text{Li}} = 19\text{ Hz}$ . This is suggestive of a bridged dimer or higher cyclic oligomer in which each carbon is coupled to two lithium atoms. The dimer structure was supported by the observation of a slope of 2.1 for the concentration dependence of the ratio of the two species ( $\log[\text{dimer}]$  vs  $\log[\text{monomer}]$ ),<sup>7</sup> and by the very similar downfield  $^{13}\text{C}$  NMR shift (7.3 ppm) of the *ipso* carbon on going from dimer to monomer compared to other ArLi reagents.<sup>8</sup>

An alternative explanation for the NMR signals could be that the 1:1:1:1 quartet corresponds to a 6-center dimeric structure with coordination to sulfur (**13**), as observed for the *N,N,N,N'*-tetramethylethylenediamine (TMEDA) complexes of 2-methyl-2-lithiodithiane (**14**)<sup>9a</sup> and phenylthiomethylithium,<sup>9b</sup> as well as several metalated phosphines.<sup>10a,b</sup> This would require that the other aggregate present be a tetramer. We consider this unlikely since the thiophene sulfur is expected to be a poor donor,<sup>11a</sup> and there is no indication of “leaning” of the sulfur toward lithium in any of the reported X-ray crystal structures of 2-lithiothiophenes<sup>4a,b</sup> or 2-lithiobenzothiophene<sup>4a</sup> or in the structure of **5B**·(THF)<sub>2</sub> reported below. The  $^{13}\text{C}$ – $^7\text{Li}$  coupling of 37.4 Hz is very similar to those of other monomeric ArLi reagents such as **4M**·PMDTA (36.3 Hz, *vide infra*), PhLi (40.4 Hz),<sup>3f,11b</sup> and 2-methoxy-6-methylphenyllithium (33.3 Hz).<sup>3d</sup>



The  $^6\text{Li}$  NMR spectrum also showed signals for the dimer and monomer at  $\delta$  1.4 and 1.1, respectively (Figure 2), but even at temperatures as low as  $-140\text{ }^\circ\text{C}$  these peaks are broadened by monomer–dimer exchange, and they coalesce near  $-131\text{ }^\circ\text{C}$ . In the  $^{13}\text{C}$  NMR spectra initial broadening occurs near  $-131\text{ }^\circ\text{C}$  and coalescence near  $-96\text{ }^\circ\text{C}$ . The  $^6\text{Li}$  and  $^{13}\text{C}$  NMR spectra for the dimer to monomer exchange were simulated and the barrier to interconversion was determined to be  $\Delta G^\ddagger_{-131} = 7.0\text{ kcal/mol}$ ,  $\Delta H^\ddagger = 5.1\text{ kcal/mol}$  and  $\Delta S^\ddagger = -13\text{ eu}$ . The barrier to dimer dissociation is significantly lower than that of PhLi ( $\Delta G^\ddagger_{-131} = 8.1\text{ kcal/mol}$  in THF).<sup>3d</sup> Similarly, the equilibrium constant for association to dimer is higher for PhLi ( $K_{\text{MD}}$  is  $210\text{ M}^{-1}$  at  $-128\text{ }^\circ\text{C}$  in 3:2 THF/Et<sub>2</sub>O) than for **1** ( $K_{\text{MD}}$  is  $2.1\text{ M}^{-1}$  at  $-136\text{ }^\circ\text{C}$  in 3:2:1 THF/Me<sub>2</sub>O/Et<sub>2</sub>O).<sup>3c,5</sup> The thermodynamic and kinetic parameters for **1** are very close to those of 2-lithio-5-methylthiophene.<sup>3e</sup>

(8) The downfield shift in the C–Li carbon on going from dimeric to monomeric aryllithiums: for **1** (7.3 ppm), **2** (8.2 ppm), **3** (9.0), **7** (11.6 ppm),<sup>3e</sup> **12** (8.8 ppm),<sup>3c</sup> and PhLi (8.2 ppm).<sup>3f,11b</sup>

(9) (a) Amstutz, R.; Seebach, D.; Seiler, P.; Schweizer, W. B.; Dunitz, J. D. *Angew. Chem., Int. Ed. Engl.* **1980**, *19*, 53. (b) Amstutz, R.; Laube, T.; Schweizer, W. B.; Seebach, D.; Dunitz, J. D. *Helv. Chim. Acta* **1984**, *67*, 224. (c) Seebach, D.; Hässig, R.; Gabriel, J. *Helv. Chim. Acta* **1983**, *66*, 308–337.

(10) (a) Engelhardt, L. M.; Jacobson, G. E.; Raston, C. L.; White, A. H. *J. Chem. Soc., Chem. Commun.* **1984**, 220. (b) Karsch, H. H.; Zellner, K.; Mikulcik, P.; Lachmann, J.; Müller, G. *Organometallics* **1990**, *9*, 190–194.

(11) (a)  $\sigma$ -Coordination of a lithium cation to the thiophene sulfur has been shown to be disfavored in lithium alkoxides. Goldfuss, B.; Schleyer, P. v. R.; Hampel, F. *Organometallics* **1997**, *16*, 5032–5041. (b) Bauer, W.; Winchester, W. R.; Schleyer, P. v. R. *Organometallics* **1987**, *6*, 2371–2379.

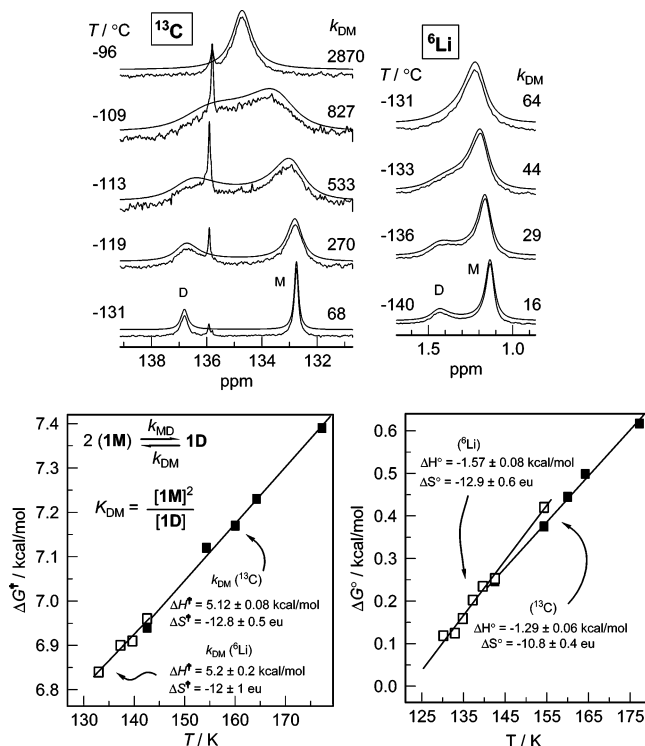


**FIGURE 2.** Variable temperature  $^{13}\text{C}$  and  $^6\text{Li}$  NMR spectra and simulations (upper lines) of the monomer–dimer coalescence of 0.15 M **1** in 3:2:1 THF/Me<sub>2</sub>O/Et<sub>2</sub>O. The Eyring and van't Hoff plots show the data obtained from both the  $^{13}\text{C}$  and  $^6\text{Li}$  spectra.

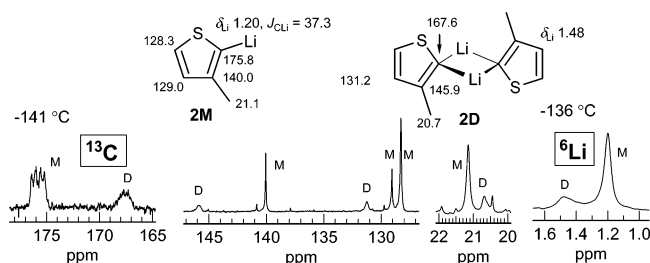


**FIGURE 3.** Low temperature  $^{13}\text{C}$  and  $^6\text{Li}$  NMR spectra of 0.14 M **2** in 3:2:1 THF/Me<sub>2</sub>O/Et<sub>2</sub>O.

**3-Methyl-2-thienyllithium (2).** Since the chelated thienyllithiums examined have an *ortho* substituent, we also investigated the solution structure of 3-methyl-2-thienyllithium (**2**). This reagent is also a mixture of monomer and dimer in 3:2:1 THF/Me<sub>2</sub>O/Et<sub>2</sub>O at low temperature. At -141 °C the  $^{13}\text{C}$  NMR spectrum (Figure 3) shows a monomer signal at  $\delta$  175.8 (1:1:1:1 quartet,  $^1J_{^{13}\text{C}-7\text{Li}} = 37.3$  Hz) and a dimer signal at  $\delta$  167.6.<sup>8</sup> A plot of  $\log[\text{dimer}]$  vs  $\log[\text{monomer}]$  for two concentrations differing by a factor of ca. 2 gave a slope of 2.0, confirming the dimer assignment.

The 3-methyl group had only a small effect on  $K_{\text{MD}}$  in **2** relative to **1**. At -136 °C,  $K_{\text{MD}}$  is 1.6 M<sup>-1</sup>, probably within experimental error of that of **1**. This is in contrast to the significant increase in dimer dissociation between PhLi ( $K_{\text{MD}} = 50$  M<sup>-1</sup>) and *o*-tolyllithium (1.7 M<sup>-1</sup>) in 4:1 THF/Et<sub>2</sub>O.<sup>3c,d</sup> The internal bond angles of the thiophene ring system ( $\angle \text{S}-\text{C}^2-\text{C}^3 = 105^\circ$  for **5**<sup>7</sup>) are smaller than in phenyllithium ( $\angle \text{C}^6-\text{C}^1-\text{C}^2 = 114^\circ$  for **10**).<sup>12</sup> The lithium environment in **1** and **2** is thus less sterically

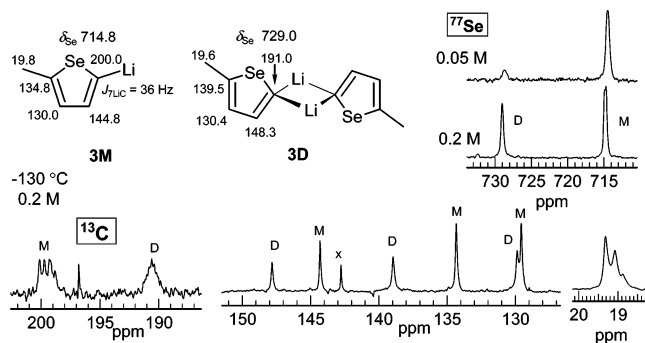


**FIGURE 4.**  $^{13}\text{C}$  and  $^{77}\text{Se}$  NMR spectra of 0.2 M **3** in 4:1 THF/Me<sub>2</sub>O at -130 °C. A  $^{77}\text{Se}$  NMR spectrum of 0.05 M **3** is also shown.

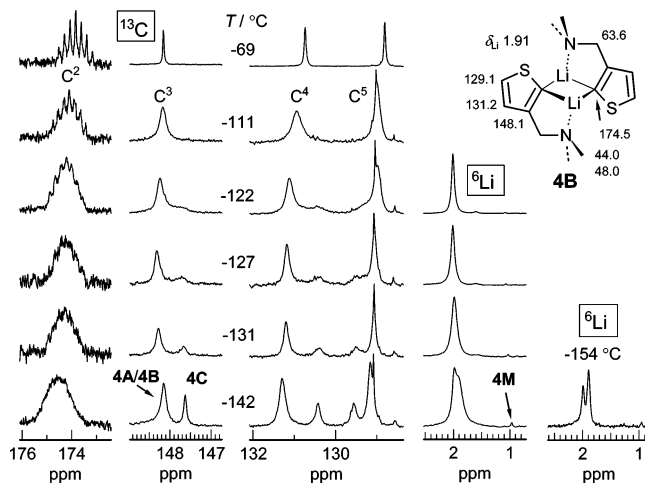


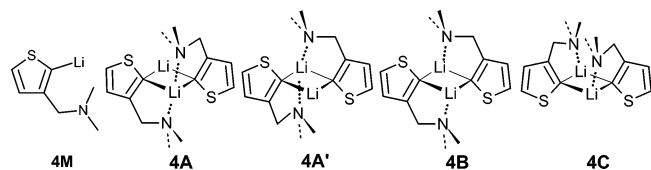
**FIGURE 5.** Variable temperature  $^6\text{Li}$  and  $^{13}\text{C}$  spectra of 0.16 M **4** in 3:2 THF/Et<sub>2</sub>O (spectra below -122 °C are in 3:2:1 THF/Et<sub>2</sub>O/Me<sub>2</sub>O).

encumbered than in PhLi and *o*-TolLi, leading to less inhibition of lithium solvation by the *o*-methyl group.

**2-Lithio-5-methylselenophene (3).** A mixture of monomer and dimer were also observed for a solution of 2-lithio-5-methylselenophene (**3**, Figure 4) in 4:1 THF/Me<sub>2</sub>O. The  $^{13}\text{C}$  shifts were substantially downfield for the monomer ( $\delta$  199.5, 1:1:1:1 quartet,  $^1J_{^{13}\text{C}-7\text{Li}} = 39$  Hz) and the dimer ( $\delta$  190.5) relative to **1** and **2**. However, the  $\Delta\delta$  (9.0 ppm) for the C-Li carbon is similar to that observed in other ArLi reagents.<sup>8</sup> The identity of the dimer was confirmed by a  $^{77}\text{Se}$  NMR variable concentration experiment (Figure 4), which produced a slope of 2.3 for a plot of  $\log[\text{dimer}]$  vs  $\log[\text{monomer}]$ .

**3-(*N,N*-Dimethylaminomethyl)-2-thienyllithium (4).** The  $^{13}\text{C}$  NMR spectrum of **4** at -142 °C (Figure 5) shows pairs of peaks for carbons C<sup>3</sup>, C<sup>4</sup>, and C<sup>5</sup> of the thiophene ring, which broaden and coalesce at higher temperatures. The signal for the carbanion carbon at  $\delta$  174.0, which is a featureless lump at low temperature because of the superposition of the signals from several chelation isomers, becomes resolved at -69 °C into a heptet ( $^1J_{^{13}\text{C}-7\text{Li}} = 15.0$  Hz) when intraaggregate exchange has become fast on the NMR time scale.<sup>3c</sup> The coupling is evident up to -30 °C, above which interaggregate exchange averages the C-Li coupling.

(12) Thoennes, D.; Weiss, E. *Chem. Ber.* **1978**, *111*, 3157–3161.

SCHEME 1. Proposed Structures of **4**

In the  $^6\text{Li}$  NMR spectra of **4** two strongly overlapped signals at  $-142\text{ }^\circ\text{C}$  eventually separate into two singlets at  $-154\text{ }^\circ\text{C}$  ( $\delta$  1.98 and 1.91). Since A-type dimers (Scheme 1) in the five-ring amine aryllithium chelates showed a  $>1.0\text{ ppm}$   $\Delta\delta$  between the two  $^6\text{Li}$  chemical shifts,<sup>3d</sup> the close proximity of these peaks suggest assignment to B- and C-type dimers. Also visible at  $-142\text{ }^\circ\text{C}$  is a small peak at  $\delta$  0.97 that has been tentatively assigned as monomer. This chemical shift is within 0.2 ppm of the monomers of **1** and **2**, and assignment as a monomer is supported by a  $^6\text{Li}$  variable concentration experiment that produced a  $\log[\text{dimer}]$  vs  $\log[\text{monomer}]$  slope of 2.4. The evidence is not strong, since the monomer is only ca. 1% of the total reagent concentration, making accurate determination of the monomer-to-dimer ratio difficult. In addition we have been unable to observe the expected 1:1:1:1 quartet for the monomer in the  $^{13}\text{C}$  NMR spectrum. In the doubly isotopically enriched compound [ $^6\text{Li},^{15}\text{N}$ ]-**4** the monomer peak appears as a singlet in the  $^6\text{Li}$  NMR spectrum. Thus, if this signal is correctly assigned, then the monomer **4M** is nonchelated unless an unusually fast exchange between **4M** and a low-concentration species that is not visible in the  $^6\text{Li}$  NMR spectrum caused loss of  $^1J_{6\text{Li}-15\text{N}}$ .

The chemical shift and coupling data for **4** are similar to those of the dimers of **1** and **2** (Table S-87), and assignment as a mixture of dimeric chelation isomers is supported by concentration independence of the species from 0.04 to 0.16 M. Although there are only two sets of signals in the  $^{13}\text{C}$  and  $^6\text{Li}/\text{Li}$  NMR spectra, several features of the spectra are inconsistent with such an assignment to just the B and C isomers. One was the observation that addition of TMEDA to **4** formed a large fraction of **4A**·TMEDA (Figure 7), which implies the presence of **4A** even in THF (vide infra).

In the low temperature  $^6\text{Li}$  spectra of  $^{15}\text{N}$ -labeled **4** the singlet at  $\delta$  1.98 in **4** becomes a doublet with  $^1J_{6\text{Li}-15\text{N}} = 2.6\text{ Hz}$  in [ $^{15}\text{N}$ ]-**4**. The second singlet at  $\delta$  1.91 becomes a small triplet with  $^1J_{6\text{Li}-15\text{N}} = 1.3\text{ Hz}$  in [ $^{15}\text{N}$ ]-**4**. This coupling is roughly half that observed in [ $^{15}\text{N}$ ]-**4A**·TMEDA (Figure 7) and is consistent with an A-type dimer where **4A** and **4A'** are undergoing rapid intramolecular exchange (Scheme 1).<sup>3b,c</sup> Since exchange between **4A** and **4A'** almost certainly goes via **4B**, this triplet corresponds to the A, A', and B isomers in rapid exchange.<sup>3a</sup> In addition, the upfield peak at  $\delta$  1.91 is much broader in both **4** and [ $^{15}\text{N}$ ]-**4** than the downfield peaks. Similarly, in the  $^{13}\text{C}$  NMR spectra (Figure 5), the major chelation isomer signals are significantly broader than those of the minor isomer. In both the  $^6\text{Li}$  and  $^{13}\text{C}$  spectra the broadening cannot be ascribed to exchange between only two species, and attempts at two-site lineshape simulation to obtain intraaggregate exchange rates failed.

We conclude that a third dimer (**4A**) is present. Reexamination of the  $-142\text{ }^\circ\text{C}$   $^{13}\text{C}$  spectrum of **4** (Figure

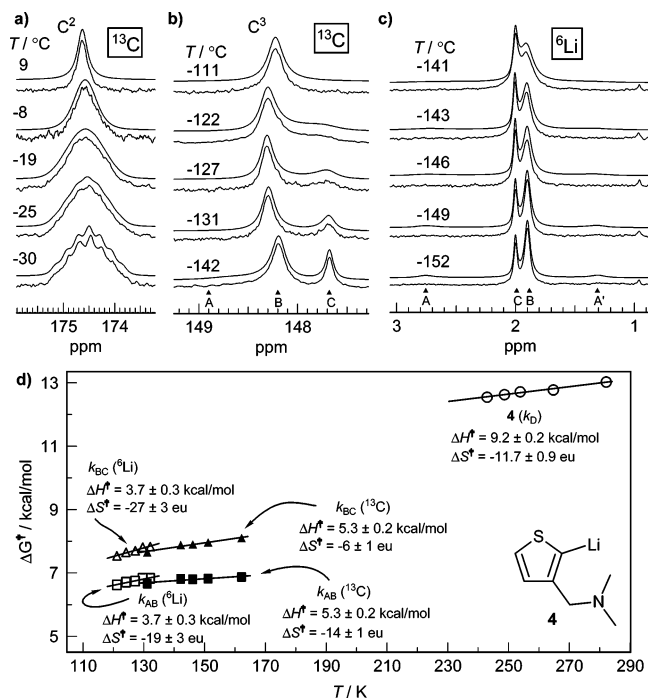


**FIGURE 6.** Variable temperature  $^{13}\text{C}$  and  $^6\text{Li}$  NMR spectra and simulations (upper lines) of **4**. (a)  $^{13}\text{C}$  NMR spectra and 7-spin simulation of interaggregate exchange (loss of  $J_{\text{CLi}}$ ,  $k_{\text{D}}$ ) of  $\text{C}^2$  (0.16 M **4** in 3:2 THF/Et<sub>2</sub>O). (b)  $^{13}\text{C}$  NMR spectra and 3-spin simulation of A/B/C dimer exchange of  $\text{C}^3$  0.16 M **4** in 3:2 THF/Et<sub>2</sub>O (spectra below  $-122\text{ }^\circ\text{C}$  are in 3:2:1 THF/Et<sub>2</sub>O/Me<sub>2</sub>O). (c)  $^6\text{Li}$  NMR spectra and 4-spin simulation of A/B/C dimer exchange of 0.13 M **4** in 3:2:1 THF/Me<sub>2</sub>O/Et<sub>2</sub>O. (d) Eyring plot of the exchange rates ( $k_{\text{D}}$  is the interaggregate exchange rate of the dimer,  $k_{\text{AB}}$ , and  $k_{\text{BC}}$  are the intraaggregate exchange rates of **4A**, **B**, and **C**).

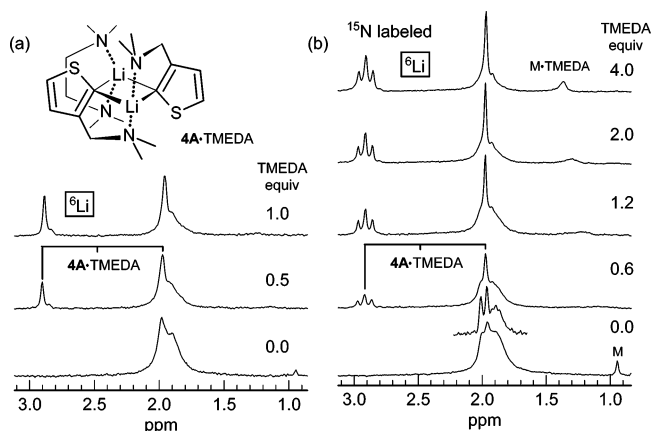


**FIGURE 7.**  $^6\text{Li}$  NMR spectra of the TMEDA titrations of 0.13M **4** ( $-141\text{ }^\circ\text{C}$ , at left) and 0.07 M [ $^6\text{Li},^{15}\text{N}$ ]-**4** ( $-144\text{ }^\circ\text{C}$ , at right) in 3:2:1 THF/Me<sub>2</sub>O/Et<sub>2</sub>O. The insert at 0 equiv of TMEDA is a Gaussian enhanced spectrum.

6b) revealed a broad shoulder downfield of the peak for **4B** at  $\delta$  148.2. We reasoned that this is **4A** (at ca.  $\delta$  148.8), near coalescence with the **4B** signal. The third signal, that of **4C** at  $\delta$  147.7, was in relatively slow exchange with the other two at  $-142\text{ }^\circ\text{C}$ . The  $^6\text{Li}$  spectrum can also be interpreted in these terms. In [ $^{15}\text{N}$ ]-**4** at  $-142\text{ }^\circ\text{C}$  the doublet at  $\delta$  1.98 with  $J_{6\text{Li}-15\text{N}} = 2.6\text{ Hz}$  can be assigned to **4C** in slow exchange, the broad peak at  $\delta$  1.91 (narrow

triplet in the  $^{15}\text{N}$  labeled compound) to the three coalesced signals of **4A**, **4A'**, and **4B**.

The variable temperature  $^{13}\text{C}$  NMR spectra could be successfully simulated on the basis of these assumptions, with the ratio of **A/B/C** at 13:62:25 and the  $k_{\text{BA}}$  exchange rate set at 9.2 times that of  $k_{\text{BC}}$ . No exchange between **4A** and **4C** was required to fully define the line shapes ( $k_{\text{AC}} = 0$ ). This is reasonable, since this process requires both a dechelation and a ring rotation, whereas interconversion of **4A** and **4B** requires only migration of N from one lithium to the other.<sup>13</sup> A  $^6\text{Li}$ -EXSY<sup>14</sup> NMR experiment on **6** showed no detectable exchange between **6A** and **6C**.<sup>3c,d</sup>

We then used the same relative rates and concentrations defined by the  $^{13}\text{C}$  simulations to calculate the  $^6\text{Li}$  line shapes (Figure 6c). In the  $-152\text{ }^\circ\text{C}$   $^6\text{Li}$  spectrum of **4**, there is a small, broad peak at  $\delta$  2.7. This peak is shifted downfield from the signals for **4B** and **4C** by a similar amount to that seen in **6A**.<sup>3a,c,d</sup> We used this peak as the chemical shift for one of the **4A** signals, and placed the other **4A** signal upfield of **4B** and **4C** by a similar amount (no peak was observed there, but the fact that the **B** signal moves very little during the **A/B** coalescence requires that the average **A/A'** shift be close to that of **B**). Although the  $^6\text{Li}$  spectra are relatively nondescript and therefore can be fit with a variety of parameters, the success in fitting the line shapes using rates and concentrations derived from the  $^{13}\text{C}$  simulation lends some strength to the assignment.

Intraaggregate exchange of **4B** and **4A** ( $k_{\text{BA}} = 240$  at  $-127\text{ }^\circ\text{C}$ ) is significantly faster than in **6** ( $k_{\text{BA}} = 2.7$  at  $-128\text{ }^\circ\text{C}$ ). Both **4** and **6** have a negative entropy of activation for the exchange rate, attributed to the association of an extra solvent molecule at the transition state to assist dechelation. Such solvent assistance would be facilitated by the less crowded steric environment in **4** compared to **6**, a consequence of the smaller intra-ring bond angles in thienyllithium.

The barrier to intermolecular aggregate exchange was estimated by performing a line-shape simulation of the collapse of the carbanion (1:2:3:4:3:2:1 heptet to a singlet, Figure 6a).<sup>7</sup> This barrier ( $\Delta G^\ddagger_{-30} = 12.1$  kcal/mol) is slightly lower than that of **6** at this temperature ( $\Delta G^\ddagger_{-30} = 12.9$  kcal/mol).<sup>3d</sup> It was not established whether the exchange was associative or dissociative.

**Interaction of 4 with TMEDA.** The TMEDA titration was crucial in establishing the solution structure of **4**. Upon addition of TMEDA, a pair of peaks in a 1:1 ratio ( $\delta$  2.9 and 1.9) appeared in the  $^6\text{Li}$  NMR spectrum (Figure 7). We assigned these peaks to TMEDA-complexed **4A**, confirmed by performing the TMEDA titration with [ $^{15}\text{N}$ ]-**4**, when the peak at  $\delta$  2.9 became a triplet with  $^1J_{^{13}\text{C}-^{15}\text{N}} = 2.9$  Hz whereas the peak at  $\delta$  1.9 was unchanged. Similar behavior was observed for **6** and **7**.<sup>3b-d</sup>

In the 2-substituted aryllithium systems, dimeric chelated aryllithium reagents only formed significant amounts of TMEDA-complexed **A**-type dimers when these were already present in THF solution (the **B** and **C** isomers cannot form a bidentate complex with TMEDA).<sup>3b-d</sup> Thus **8** and the pyrrolidine analogue of **6** (**10**), which show only

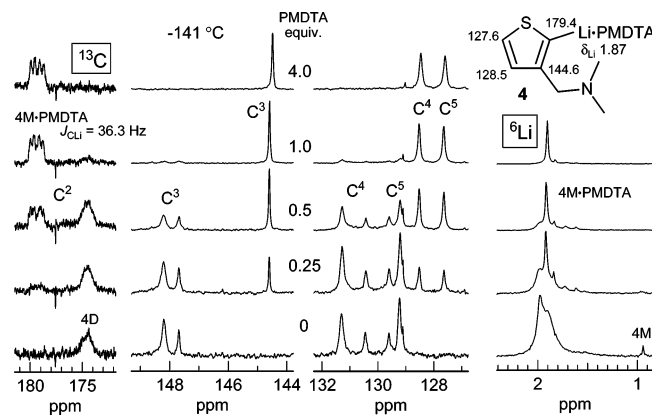


**FIGURE 8.**  $^{13}\text{C}$  and  $^6\text{Li}$  NMR spectra of the PMDTA titration of 0.14 M **4** in 3:2:1 THF/Me<sub>2</sub>O/Et<sub>2</sub>O at  $-141\text{ }^\circ\text{C}$ .

a single chelation isomer in THF (probably of the **B**-type),<sup>3g</sup> did not interact significantly with TMEDA, whereas **6** and **7**, which each have an **A**-type dimer present in solution, formed significant amounts of **A**-type TMEDA adducts. In other words, the thermodynamic driving force for complexation of TMEDA to the **A**-isomer is not very large, consistent with the relatively close energetic balance between THF and TMEDA complexation to lithium seen in other contexts.<sup>15a</sup> Thus the formation of **4A**·TMEDA implies that a significant fraction of **4A** was present. As discussed above, this provided an important clue as to the correct assignment of the THF spectra.

**Interaction of 4 with PMDTA.** The tridentate ligand PMDTA (*N,N,N',N'',N'''*-pentamethyldiethylenetriamine) is often effective at dissociating dimers to monomers.<sup>3b-d,f,11b,16</sup> Depending on the strength of chelation, it can also have the effect of reducing or entirely blocking chelation, since a PMDTA-coordinated chelated lithium reagent would have a sterically crowded pentacoordinated lithium. The chelated aryllithium reagents **6–9** show a range of behaviors, with the dimer of **6** undergoing only bidentate coordination to PMDTA, even when in large excess, signaling a very strong dimerization and chelation;<sup>3d</sup> **8** is deaggregated to monomer by PMDTA, but the methoxy group is still weakly chelated in the complex, whereas **7** and **9** (as well as nonchelated analogues) are fully deaggregated and dechelated by PMDTA.<sup>3b,c</sup> Thus the interaction with PMDTA provides a qualitative measure of the strength of chelation, with **6** > **8** > **9** > **7**.

The PMDTA titration of **4** (Figure 8) shows that the dimers readily dissociated to PMDTA-complexed monomers in a nearly stoichiometric fashion, with a new carbanion signal in the  $^{13}\text{C}$  NMR spectra at  $\delta$  179.5 (1:1:1:1 quartet,  $^1J_{^{13}\text{C}-^{7}\text{Li}} = 36.3$  Hz) and new signals for C<sup>2</sup>, C<sup>3</sup>, and C<sup>4</sup> of the thiophene ring. A new  $^6\text{Li}$  NMR signal at  $\delta$  1.88, 0.9 ppm downfield from the THF-complexed monomer at  $\delta$  0.97, was also observed. PMDTA complexation typically causes a ca. 1 ppm downfield shift of the lithium signal in monomeric lithium reagents.<sup>3c</sup>

(15) (a) Collum, D. B. *Acc. Chem. Res.* **1992**, *25*, 448–454. (b) Romesberg, F. E.; Gilchrist, J. H.; Harrison, A. T.; Fuller, D. J.; Collum, D. B. *J. Am. Chem. Soc.* **1991**, *113*, 5751–5757.

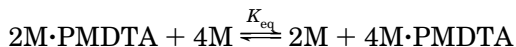
(16) Lappert, M. F.; Engelhardt, L. M.; Raston, C. L.; White, A. H. *J. Chem. Soc., Chem. Commun.* **1982**, 1323–1324. Fraenkel, G.; Chow, A.; Winchester, W. R. *J. Am. Chem. Soc.* **1990**, *112*, 6190–6198. Fraenkel, G.; Subramanian, S.; Chow, A. *J. Am. Chem. Soc.* **1995**, *117*, 6300–6307.

(13) We note, however, that in 2-diethylaminophenyllithium the **B/C** exchange is substantially faster than the **A/B** exchange.<sup>3d</sup>

(14) Perrin, C. L.; Dwyer, T. *J. Chem. Rev.* **1990**, *90*, 935–967.

The complete dissociation to monomer is in sharp contrast to the phenyl analogue **6**, which showed no detectable monomer formation with excess PMDTA.<sup>3d</sup> The weaker chelation in **4** is surprising (it matches more closely that of **7**<sup>3b,c</sup>) given that the systems are both aromatic five-ring amine chelates. On the basis of the similar  $K_{MD}$  values for **2** and *o*-TolLi, one might predict that chelation in **4** and **6** would be comparable.

**Competitive PMDTA Titration.** Further insight into the chelation properties of the monomer and dimers of **4** was provided by comparing the PMDTA-affinity of **2** and **4**. If, as suggested by the absence of Li–N coupling in the NMR studies, the monomer is not chelated, PMDTA should show little preference for binding to either **2M** or **4M**. Substoichiometric quantities of PMDTA were added to an equimolar solution of **2** and **4** at  $-143\text{ }^{\circ}\text{C}$ , and the concentrations of the observable species (**2M**, **2M**·PMDTA, **4B**, **4C**, and **4M**·PMDTA) were determined by line shape fitting of the <sup>13</sup>C NMR spectra. The concentrations of **2D** and **4M** (which were not observed directly) were calculated from previously determined  $K_{MD}$  values).  $K_{eq}$  was calculated to be 1.8 at  $-143\text{ }^{\circ}\text{C}$ . Thus formation of **4M**·PMDTA is actually slightly favored over formation of **2M**·PMDTA relative to their respective monomeric THF complexes. We interpret this as direct evidence that **4M** is weakly chelated or unchelated.



**Interaction of **4** with HMPA.** Hexamethylphosphoric triamide (HMPA) is a strong donor solvent with the ability to deaggregate and ion-separate many kinds of lithium reagents. The advantageous NMR properties (particularly the observation of <sup>7</sup>Li–<sup>31</sup>P *J* coupling) has allowed HMPA to be used as a detailed probe of solution structure (including solvation state, aggregation state, and ion pair status) of many lithium species.<sup>3h,15b,17</sup> In the aryllithium series, NMR analysis of the interaction with HMPA provides an indirect measure of chelation strength,<sup>3a–d</sup> since HMPA is able to displace solvent and sometimes chelating groups from the lithium atom. The HMPA titration of **4** is presented in Figure 9. Interpretation of these spectra is made difficult by the exceptionally small <sup>7</sup>Li chemical shift changes between chelation isomers as well as between the HMPA- and THF-solvated dimers, and also by the poorly resolved coupling in the <sup>7</sup>Li spectrum, due to the unusually short <sup>7</sup>Li  $T_1$ .<sup>15</sup> Despite these problems, the HMPA titrations of **4** did yield some information.

(17) HMPA Normant, H. *Angew. Chem., Int. Ed. Engl.* **1967**, *6*, 1046. Dolak, T. M.; Bryson, T. A. *Tetrahedron Lett.* **1977**, 1961–1964. Carlier, P. R.; Lo, C. W.-S. *J. Am. Chem. Soc.* **2000**, *122*, 12819–12823. Denmark, S. E.; Swiss, K. A. *J. Am. Chem. Soc.* **1993**, *115*, 12195–12196. Fraenkel, G.; Hallden-Abberton, M. P. *J. Am. Chem. Soc.* **1981**, *103*, 5657–5664. Abatjoglou, A. G.; Eliel, E. L.; Kuyper, L. F. *J. Am. Chem. Soc.* **1977**, *99*, 8262. Lucchetti, J.; Krief, A. *J. Organomet. Chem.* **1980**, *194*, C49.

(18) (a) For many organolithium reagents, especially aggregated ones, quadrupolar broadening is severe enough with <sup>7</sup>Li (92.6% natural abundance) that C–Li coupling cannot be well resolved. The <sup>6</sup>Li analogues show little or no quadrupolar broadening and thus couplings are more easily seen. Fraenkel, G.; Fraenkel, A. M.; Geckle, M. J.; Schloss, F. J. *J. Am. Chem. Soc.* **1979**, *101*, 4745–4747. (b) A broad doublet is seen for <sup>13</sup>C or <sup>31</sup>P signals coupled to one <sup>7</sup>Li when  $T_1$  relaxation becomes comparable to  $1/J_{X-Li}$  as a result collapse of the outer pairs of the 1:1:1:1 quartet. Sometimes the 1:1:1 triplet due to the natural abundance <sup>6</sup>Li visible in the valley of the doublet.<sup>11b</sup> Bacon, J.; Gillespie, R. J.; Quail, J. W. *Can. J. Chem.* **1963**, *41*, 3063–3069.

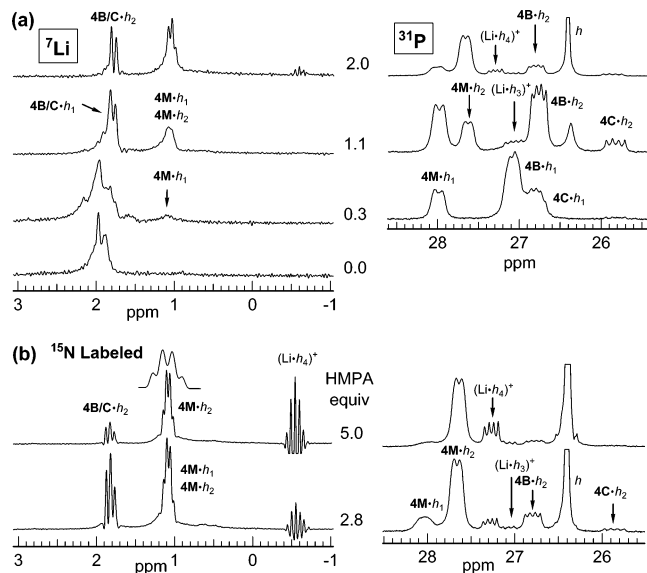


**FIGURE 9.** <sup>7</sup>Li and <sup>31</sup>P NMR spectra of the HMPA titration of **4** in 3:2:1 THF/Me<sub>2</sub>O/Et<sub>2</sub>O. The assignments for **4B** and **4C** could be reversed. (a) 0.04 M solution of natural abundance **4** at  $-143\text{ }^{\circ}\text{C}$ . (b) 0.23 M solution of <sup>15</sup>N-labeled **4** at  $-141\text{ }^{\circ}\text{C}$ .

The addition of HMPA initially produced three new mono-HMPA complexed species, assigned in the <sup>31</sup>P NMR spectrum as a monomer (**4M**·*h*<sub>1</sub>) at  $\delta$  28.0 and two dimers (**4B**·*h*<sub>1</sub> and **4C**·*h*<sub>1</sub>) at  $\delta$  27.1 and 26.6, respectively. The 1:1:1:1 quartets expected for **4M**·*h*<sub>1</sub> and **4B**·*h*<sub>1</sub> are collapsed to pseudo-doublets by <sup>7</sup>Li quadrupolar relaxation.<sup>15b</sup> At higher equivalents of HMPA three new bis-HMPA solvates are formed: **4M**·*h*<sub>2</sub> at  $\delta$  27.7, **4B**·*h*<sub>2</sub> at  $\delta$  26.6, and **4C**·*h*<sub>2</sub> at  $\delta$  25.8. Coupling to <sup>7</sup>Li is apparent in **4B**·*h*<sub>2</sub> ( $^2J_{31P-7Li} = 8.3\text{ Hz}$ ) and **4C**·*h*<sub>2</sub> ( $^2J_{31P-7Li} = 11.0\text{ Hz}$ ). A <sup>31</sup>P signal for excess HMPA at  $\delta$  26.4 is visible above 1 equiv, and low concentrations of the tris- and tetrakis-HMPA solvated separated ions Li·*h*<sub>3</sub><sup>+</sup> and Li·*h*<sub>4</sub><sup>+</sup> are seen in the <sup>7</sup>Li and <sup>31</sup>P NMR spectra. Such signals are usually due to the presence of triple ion (Ar<sub>2</sub>Li·Li(HMPA)<sub>2</sub>)<sub>2</sub><sup>+</sup>,<sup>31</sup> although in this case the lithium signal of the Ar<sub>2</sub>Li<sup>+</sup> group, which is usually quite broad in the <sup>7</sup>Li NMR spectrum and appears near  $\delta$  3, was not detected. At 2 equiv of HMPA, **4** was converted to less than 4% of separated ions.

An HMPA titration of [<sup>15</sup>N]-**4** (Figure 9b) showed that the final HMPA complexes were all chelated, since each of the <sup>7</sup>Li NMR signals now showed an additional splitting. Thus the superimposed dimer signals of **4B**·*h*<sub>2</sub> and **4C**·*h*<sub>2</sub> were now a doublet of doublets, and the signals of **4M**·*h*<sub>1</sub> and **4M**·*h*<sub>2</sub> were now a triplet and quartet ( $J = 5.9\text{ Hz}$ ), respectively, due to the near equivalence of  $^2J_{Li-P}$  and  $^1J_{Li-N}$ . A similar result was observed for the phenyl analogues [<sup>6</sup>Li,<sup>15</sup>N]-**6** and [<sup>6</sup>Li,<sup>15</sup>N]-2-methoxy-6-(*N,N*-dimethylaminomethyl)phenyllithium.<sup>3a,d</sup>

**3-Methoxymethyl-2-thienyllithium (**5**).** Unlike **4**, **5** is mostly monomeric in THF at low temperatures, as seen from the 1:1:1:1 quartet ( $J_{13C-7Li} = 37.6\text{ Hz}$ ) at  $\delta$  182.1 in the <sup>13</sup>C NMR spectrum at  $-146\text{ }^{\circ}\text{C}$  (Figure 10). There is also a higher aggregate present (C–Li signal at  $\delta$  177.2). We were unable to obtain Li–C coupling for this species because of the low barrier to aggregate interconversion, which averages the coupling (the monomer loses coupling above  $-146\text{ }^{\circ}\text{C}$ ), nor were we able to confirm

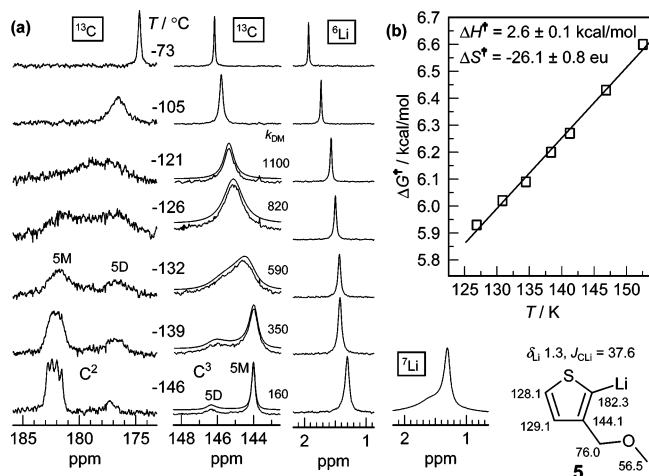


**FIGURE 10.** (a) Variable temperature  $^{13}\text{C}$ ,  $^6\text{Li}$ , and  $^7\text{Li}$  NMR spectra of 0.14 M **5** in 3:2:1 THF/Me<sub>2</sub>O/Et<sub>2</sub>O of monomer–dimer coalescence. Simulated line shapes of the  $^{13}\text{C}$  NMR spectra are shown above the corresponding spectrum. (b) Eyring plot of the monomer–dimer coalescence.

the aggregation state by a dilution study because of the low aggregate concentration and low reagent solubility. A dimer structure is supported by the carbanion chemical shift of  $\delta$  177.2<sup>8</sup> and the crystallization from THF of a B-type THF-solvated dimer whose structure was determined by X-ray diffraction (vide infra). At higher temperatures the averaged  $^{13}\text{C}$  and  $^7\text{Li}$  signals at  $-73$  °C were close to those of the dimer, so the fraction of aggregate is higher at higher temperatures, as also observed for several other aryl and vinyl lithium monomer–dimer<sup>3c,19</sup> and dimer–tetramer<sup>9c,20</sup> pairs.

The  $^{13}\text{C}$  NMR signals of **5M** and **5D** for C<sup>3</sup> ( $\delta$  145) coalesce near  $-126$  °C, giving  $\Delta G^\ddagger_{-121} = 6.6$  kcal/mol for the dimer to monomer interconversion in 3:2:1 THF/Me<sub>2</sub>O/Et<sub>2</sub>O, substantially lower than the barrier for **8**,  $\Delta G^\ddagger_{-121} = 8.5$  kcal/mol, measured in a slightly different solvent mixture (3:2:1 Me<sub>2</sub>O/THF/Et<sub>2</sub>O).<sup>3c</sup> The ca. 2 kcal difference is similar to that between **1** and PhLi. We were unable to decoalesce the monomer and dimer signals in the  $^6\text{Li}$  NMR spectrum even at  $-146$  °C; however, the  $^7\text{Li}$  spectrum (Figure 10a) shows a broad downfield peak, which is consistent with partially coalesced signals of the monomer and dimer. Line shape simulations of both the  $^6\text{Li}$  and  $^7\text{Li}$  spectra using the rate of monomer interconversion and the dimer-to-monomer ratio determined from the  $^{13}\text{C}$  NMR spectra along with an estimation of the dimer  $^7\text{Li}$  chemical shift ( $\delta$  1.64) gave a reasonable fit.

**Solid State Structure of 5.** We were able to obtain a single-crystal X-ray structure of the THF-solvated B-type dimer of **5** (Figure 11). This is the first published structure of a chelated 2-thienyllithium reagent,<sup>3e,4b,a</sup> although there is a private communication of such a structure in the Cambridge Structural Database, the TMEDA complex of **4** (structure shown in Figure 7).<sup>4b</sup> The centrosymmetric structure of **5B**·(THF)<sub>2</sub> shows the pendant ether moiety in close proximity (1.95 Å) to the

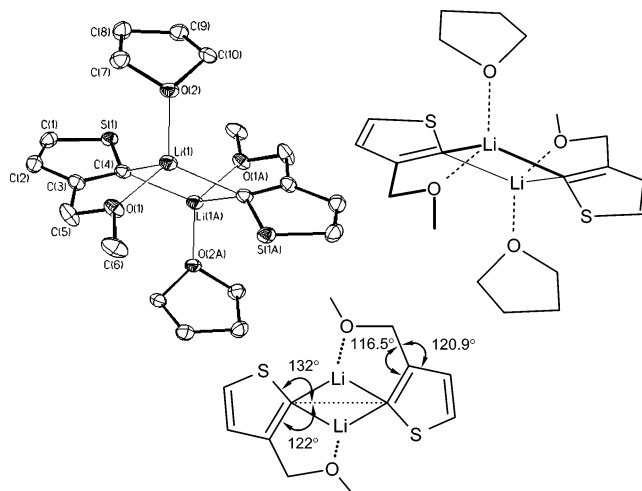


**FIGURE 11.** Single-crystal X-ray structure of **5B**·(THF)<sub>2</sub>. Hydrogens omitted for clarity.

bridging lithium atom and bonded almost trigonally (sum of angles around O is 358°). Each lithium is tetracoordinate, with a molecule of THF completing the solvation shell. The coordinated THF is bonded on the “endo” lone pair, as is commonly seen in THF solvates, approximately 50% toward tetrahedral (sum of angles around O is 341.6°, tetrahedral is 328.5°) with an O–Li bond length identical to that of the chelating methoxy group. The central CLiCLi ring is normal for structures of this type: planar with C–Li bond distances of 2.16 and 2.22 Å, a C–Li–C bond angle of 112° and Li–C–Li angle of 68°. There is no indication of S–Li coordination (the Li–S distance is 3.70 Å), since the thiophene ring actually has the S tilted away from the Li, as shown in Figure 11 (S–C···C angle of 132° vs C–C···C angle of 122°). This distortion also moves the chelating group toward the lithium. Similarly, the C–CH<sub>2</sub> bond is bent toward the lithium, whereas most 3-alkyl-substituted thiophenes have the exocyclic bond bent the other way (away from the sulfur).<sup>21</sup> The thiophene rings are planar, with the plane tilted 54° from the CLiCLi plane.

One hypothesis proposed for the correlation between aggregation and chelation involves the C–Li–X bite angle (where X is a solvent molecule or chelating atom).<sup>3c,i</sup> If the bite angle is smaller, there is expected to be less cancellation of the Li–C dipole by the Li–X dipole and thus a higher propensity for dimerization, which cancels this dipole. The O(1)–Li(1)–C(4) bite angle in **5B**·(THF)<sub>2</sub> is 85.3°, nearly identical to the C–Li–N bite angle of 85.9° in **10B**·(THF)<sub>2</sub>,<sup>3g</sup> which is much more strongly dimerized. This weakens the hypothesis but the comparison is imperfect because of the different chelating groups and the higher basicity of the phenyl anion ( $pK_a$  of benzene ca. 43<sup>22a</sup>) compared to the thienyl anion ( $pK_a$  of thiophene ca. 38<sup>22b</sup>).

**Interaction of 5 with TMEDA.** The addition of TMEDA to **5** at  $-139$  °C generated a new set of  $^{13}\text{C}$  signals corresponding to the TMEDA-complexed mono-

(19) Knorr, R.; Freudenreich, J.; Polborn, K.; Nöth, H.; Linti, G. *Tetrahedron* **1994**, *50*, 5845–5860.

(20) Bauer, W.; Griesinger, C. *J. Am. Chem. Soc.* **1993**, *115*, 10871–10882.

(21) For example, in 1,6-bis(3-thienyl)hexane: Chaloner, P. A.; Gunatunga, S. R.; Hitchcock, P. B. *J. Chem. Res.* **1997**, 267.

(22) (a) Streitwieser, A., Jr.; Scannon, P. J.; Niemeyer, H. M. *J. Am. Chem. Soc.* **1972**, *94*, 7936–7937. (b) Streitwieser, A., Jr.; Scannon, P. J. *J. Am. Chem. Soc.* **1973**, *95*, 6273–6276.

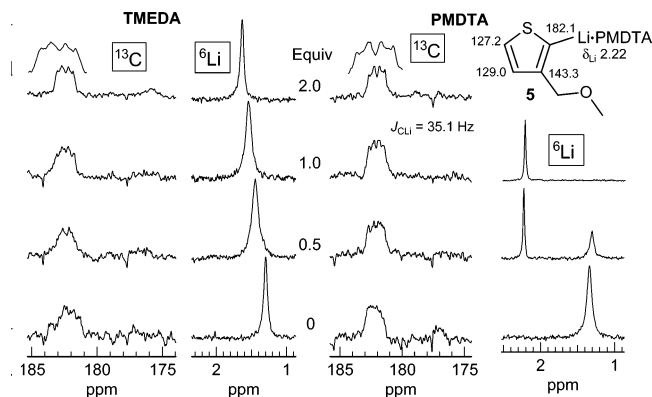


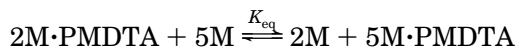
**FIGURE 12.** TMEDA (0.13 M,  $-139\text{ }^{\circ}\text{C}$ ) and PMDTA (0.14 M,  $-143\text{ }^{\circ}\text{C}$ ) titrations of **5** in 3:2:1 THF/Me<sub>2</sub>O/Et<sub>2</sub>O.

mer (C–Li carbon at  $\delta$  182.4, 1:1:1:1 quartet,  $^1J_{^{13}\text{C}-^7\text{Li}} = 36\text{ Hz}$ , Figure 12). The  $^6\text{Li}$  spectrum did not show a new peak, instead the averaged monomer–dimer peak gradually moved downfield as more TMEDA was added. This peak, which was significantly broadened by exchange between the species at  $-142\text{ }^{\circ}\text{C}$ , decoalesced at lower temperatures to TMEDA-solvated ( $\delta$  1.75) and THF-solvated ( $\delta$  1.3) monomer signals. Monomeric TMEDA complexes of other aryllithium reagents have also shown a very high lability to ligand exchange.<sup>3c,d</sup>

**Interaction of **5** with PMDTA.** The addition of PMDTA to **5** quantitatively converted the monomer and dimer to PMDTA-complexed monomer at  $-143\text{ }^{\circ}\text{C}$  (Figure 12). The carbanion of the PMDTA-complexed monomer appears at  $\delta$  182.1 as a 1:1:1:1 quartet ( $^1J_{^{13}\text{C}-^7\text{Li}} = 35.1\text{ Hz}$ ), overlapping the THF-solvated monomer. The  $^6\text{Li}$  NMR spectrum shows the new monomer at  $\delta$  2.2. This new peak is significantly sharper than the peak we have assigned as the averaged monomer–dimer peak ( $\delta$  1.3), which supports the assignment made above that the THF-solvated monomer and dimer are exchanging on the NMR time scale.

A dynamic NMR study of a series of ArLi–PMDTA complexes, including PhLi, *o*-ethylphenyllithium, and *o*-(3-methoxypropyl)phenyllithium, showed very similar behavior for the symmetrization and complexation-decomplexation dynamics of the PMDTA ligand.<sup>3c</sup> However, the PMDTA complex of **8** was much more labile than the others, leading to the conclusion that **8** is still chelated even when complexed with PMDTA (pentacoordinate lithium). No such behavior was shown by **5**·PMDTA, which was much like that of unchelated model systems. We conclude that **5**·PMDTA is nonchelated. Thus, as observed for the amine analogue **4**, chelation in **5** is weaker than in the phenyl analogue.

**Competitive PMDTA Experiment.** A competitive PMDTA titration was also performed on **2** and **5**.<sup>7</sup> Addition of 0.6 equiv of PMDTA resulted in the formation of **2M**·PMDTA and **5M**·PMDTA in a 1.2:1 ratio. In the  $^{13}\text{C}$  NMR spectrum, the signals for C<sup>3</sup> of **2M**·PMDTA and **5M**·PMDTA appeared upfield of the THF-solvated monomers by ca. 0.5 ppm. In the  $^6\text{Li}$  NMR spectrum, the signals for **2M**·PMDTA and **5M**·PMDTA were observed at  $\delta$  2.24 and 2.13, respectively.  $K_{\text{eq}}$  was determined to be 1.6, comparable to the  $K_{\text{eq}}$  value of 1.8 measured for the competitive PMDTA titration of **2** and **4**. It appears that **5M**, like **4M**, is not chelated.



**Interaction of **5** with HMPA.** The HMPA titration of **5** is shown in Figure 13. Addition of 1 equiv of HMPA resulted in the stoichiometric formation of a monomeric complex **5M**·*h*<sub>1</sub>, seen as a doublet at  $\delta$  1.2 ( $^2J_{^7\text{Li}-^{31}\text{P}} = 8.8\text{ Hz}$ ) in the  $^7\text{Li}$  NMR spectrum and a broad doublet at  $\delta$  27.5 in the  $^{31}\text{P}$  NMR spectrum.<sup>18b</sup> In contrast, the dimer of **8** was still present in low concentration at 4 equiv of HMPA.<sup>3c</sup> Also unusual is the early appearance (1.5 equiv HMPA) of signals for the ate-complex Ar<sub>2</sub>Li<sup>−</sup>Li(HMPA)<sub>4</sub><sup>+</sup> in both the  $^7\text{Li}$  ( $\delta$   $-0.17, 2.5$ ) and  $^{31}\text{P}$  ( $\delta$  27.3) spectra. The contact ion pair **5M**·*h*<sub>2</sub> also appears at 1.5 equiv HMPA as a triplet at  $\delta$  0.95 in the  $^7\text{Li}$  NMR spectrum and a pseudo-doublet<sup>18b</sup> at  $\delta$  26.9 in the  $^{31}\text{P}$  NMR spectrum. The  $^{13}\text{C}$  NMR spectrum showed two carbanion carbon signals at  $\delta$  184.2 ( $^1J_{^{13}\text{C}-^7\text{Li}} = 34.9\text{ Hz}$ ) and  $\delta$  187.2 ( $^1J_{^{13}\text{C}-^7\text{Li}} = 32.5\text{ Hz}$ ) corresponding to **5M**·*h*<sub>1</sub> and **5M**·*h*<sub>2</sub>, respectively. The free HMPA seen in solution ( $\delta$  26.4) is due to the low association constant of **5M**·*h*<sub>1</sub> for a second HMPA molecule.

## Summary

In the 2-thienyllithium systems that contain potential five-membered ring chelating groups (**4** and **5**), chelation is clearly much weaker than in the phenyl analogues **6** and **8**. In fact, **5** shows no indication of any chelation. For each system *N,N*-dimethylaminomethyl is a stronger chelating group than methoxymethyl. We propose that one factor responsible for the lower chelation strength in thiophene is the smaller ring size and resulting larger external bond angles that orient the C–Li bond further away from the chelating substituent than in the phenyl system. The increased distance between the lithium atom and the chelating group weakens their interaction. Smaller steric hindrance around the C–Li bond would also rationalize the small effect that introduction of an *o*-methyl group (**1** to **2**, Table 1) has on the monomer dimer equilibrium.

This effect also helps explain why the barriers to interconversion of the dimer chelation isomers in **4** are lower than in the corresponding phenyllithium analogue (**6**). The negative entropy of activation for intramolecular exchange suggests that coordination of an extra solvent molecule is required to break the chelation, a process facilitated by the less sterically hindered lithium environment in the thiophene system.

The correlation seen in the aryllithium systems between chelation and aggregation<sup>3c,d</sup> holds for compounds **2**, **4**, and **5** as well. Compound **4** is chelated and also substantially aggregated ( $K_{\text{MD}} = 15,900\text{ M}^{-1}$ ), whereas **5** shows essentially the same level of aggregation ( $K_{\text{MD}} = 3.3\text{ M}^{-1}$ ) as the model compound **2** ( $K_{\text{MD}} = 1.6\text{ M}^{-1}$ ) and little sign of chelation, as judged from the behavior toward PMDTA and the negligible  $\Delta\delta$  ( $<1\text{ ppm}$ ) observed for both the OCH<sub>3</sub> and CH<sub>2</sub>OMe  $^{13}\text{C}$  chemical shifts in the THF, PMDTA, and HMPA-complexed monomers. The absence of chelation in **5** is a caution for chemists who have routinely assumed that appropriately situated chelating groups (especially those capable of forming five-membered rings) will form chelate rings.

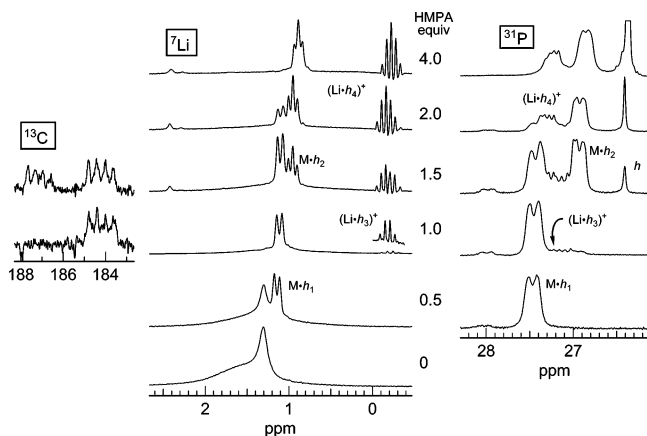


**FIGURE 13.**  $^7\text{Li}$  and  $^{31}\text{P}$  NMR spectra of the  $-145\text{ }^\circ\text{C}$  HMPA titration of 0.13 M **5** in 3:2:1 THF/Me<sub>2</sub>O/Et<sub>2</sub>O ( $h$  = HMPA).

**TABLE 1.** Thermodynamic and Kinetic Data for Chelated Aryllithiums and Model Compounds

$$2 \text{ M} \xrightleftharpoons[k_{\text{DM}}]{k_{\text{MD}}} \text{D}$$

$$K_{\text{MD}} = \frac{k_{\text{MD}}}{k_{\text{DM}}} = \frac{[\text{D}]}{[\text{M}]^2}$$

compd	R	$K_{\text{MD}}$ (M <sup>-1</sup> )	$\Delta G^a$ (T, °C)	$\Delta G_{\text{DM}}^{\ddagger a}$ (T, °C)
<b>1</b>	H	2.1	-0.2 (-136) <sup>b</sup>	7.0 (-131) <sup>b,c</sup>
<b>2</b>	CH <sub>3</sub>	1.6	-0.1 (-136) <sup>b</sup>	7.2 (-131) <sup>b,c</sup>
<b>4</b>	CH <sub>2</sub> NMe <sub>2</sub>	15,900	-2.6 (-141) <sup>b</sup>	12.1 <sup>d</sup> (-30) <sup>e</sup>
<b>5</b>	CH <sub>2</sub> OMe	3.3	-0.3 (-135) <sup>b</sup>	6.6 (-121) <sup>b,c</sup>
Ph	H <sup>f</sup>	210	-1.5 (-128) <sup>e</sup>	8.3 (-101) <sup>e,g</sup>
Ph	CH <sub>3</sub> <sup>f</sup>	1.7	-0.2 (-135) <sup>h</sup>	
<b>6</b>	CH <sub>2</sub> NMe <sub>2</sub> <sup>i</sup>	> 17,000	≤ -2.6 (-131) <sup>e</sup>	> 12.5 <sup>d,j</sup> (-36) <sup>e</sup>
<b>8</b>	CH <sub>2</sub> OMe <sup>k</sup>	> 35,400	≤ -3.0 (-127) <sup>e</sup>	≥ 9.5 <sup>d</sup> (-80) <sup>l</sup>

<sup>a</sup> Free energies in kcal/mol for  $k_{\text{DM}}$  and  $K_{\text{DM}}$ .  $\Delta G$  is the free energy difference between a dimer and two molecules of monomer. <sup>b</sup> 3:2:1 THF/Me<sub>2</sub>O/Et<sub>2</sub>O. <sup>c</sup> Exchange of monomer and dimer signals in  $^6\text{Li}$  and  $^{13}\text{C}$  NMR spectra. <sup>d</sup> Coalescence of the 1:2:3:2:1 quintet of the C-Li carbon. <sup>e</sup> 3:2 THF/Et<sub>2</sub>O. <sup>f</sup> Phenyllithium, ref 3f. <sup>g</sup> THF. <sup>h</sup> 4:1 THF/Et<sub>2</sub>O. <sup>i</sup> Reference 3d. <sup>j</sup> The rate is bimolecular. <sup>k</sup> 3:2:1 Me<sub>2</sub>O/THF/Et<sub>2</sub>O. <sup>l</sup> Reference 3c.

## Experimental Section

**NMR Spectroscopy.** All low-temperature multinuclear NMR experiments were conducted on a spectrometer equipped with a 10 mm wide-bore broadband probe at the following frequencies: 360.148 MHz ( $^1\text{H}$ ), 90.556 MHz ( $^{13}\text{C}$ ), 52.984 MHz ( $^6\text{Li}$ ), 139.905 MHz ( $^7\text{Li}$ ), and 145.785 MHz ( $^{31}\text{P}$ ).

All spectra were taken of samples in a combination of the protio solvents THF, ether, and/or Me<sub>2</sub>O with the spectrometer unlocked. Sample temperatures in NMR experiments were measured using the internal  $^{13}\text{C}$  chemical shift thermometer tris(trimethylsilyl)methane enriched 10% with  $^{13}\text{C}$ .<sup>3j</sup>

**Dynamic NMR Simulation.** Many of the variable temperature NMR spectra were simulated to determine rate constants, activation parameters, and/or peak areas. These simulations were performed with the computer program WINDNMR,<sup>3k</sup> using one of the standard exchange matrices (random exchange of singlets) or custom setups for more complex situations.

**2-Thienyllithium (1).** A solution of *n*-BuLi in hexanes (2.45 M, 0.20 mL, 0.49 mmol) was added to a dry, N<sub>2</sub>-purged 10-mm NMR tube containing a solution of thiophene (41.6 mg, 0.49 mmol) in THF (1.5 mL) at  $-78\text{ }^\circ\text{C}$ . The solution was stored overnight at  $-78\text{ }^\circ\text{C}$ , and dry Me<sub>2</sub>O (1.0 mL), Et<sub>2</sub>O (0.5 mL) and (Me<sub>3</sub>Si)<sub>3</sub>CH (1  $\mu\text{L}$ )<sup>3j</sup> were added immediately before the

variable temperature NMR experiment. Spectra and data are reported in Figures 1 and 2 and Tables S-1 and S-2.<sup>7</sup> After the experiment, the sample was quenched with Me<sub>3</sub>SiCl (75  $\mu\text{L}$ , 0.58 mmol) and stored overnight at  $-78\text{ }^\circ\text{C}$ . 2-Trimethylsilylthiophene was extracted with 1:1 Et<sub>2</sub>O/hexane, the organic layer washed with brine, dried with MgSO<sub>4</sub>, and filtered, and the solvent removed in vacuo. 2-(Trimethylsilyl)thiophene was recovered in 77% yield based on integration vs pentachloroethane (30  $\mu\text{L}$ , 0.25 mmol) in the  $^1\text{H}$  NMR spectrum.

**3-Methyl-2-thienyllithium (2).** 3-Methyl-2-trimethylstannylthiophene (**15**, 110 mg, 0.43 mmol) was added to a dry, N<sub>2</sub>-purged 10-mm NMR tube sealed with a septum. THF (1.5 mL) was added, and the solution was cooled to  $-78\text{ }^\circ\text{C}$ . *n*-BuLi (2.5 M, 0.18 mL, 0.43 mmol) was added slowly, and the sample was mixed by shaking the NMR tube. The sample was stored at  $-78\text{ }^\circ\text{C}$  for 3 h. Me<sub>2</sub>O (1.0 mL), Et<sub>2</sub>O (0.5 mL), and (Me<sub>3</sub>-Si)<sub>3</sub>CH (2  $\mu\text{L}$ )<sup>3j</sup> were added. A series of  $^{13}\text{C}$  and  $^6\text{Li}$  NMR spectra were acquired between  $-136$  and  $-109\text{ }^\circ\text{C}$ . Spectra and data are reported in Figures 3 and S-1 and Table S-3.<sup>7</sup> The sample was quenched with Me<sub>3</sub>SiCl (80  $\mu\text{L}$ , 0.63 mmol), diluted with 1:1 Et<sub>2</sub>O/hexane, and washed with H<sub>2</sub>O and brine. The organic layer was dried with MgSO<sub>4</sub>, filtered, and concentrated. The quantity of the resulting silane (0.36 mmol, 84%) was determined by integration relative to pentachloroethane (30  $\mu\text{L}$ , 0.25 mmol) in the  $^1\text{H}$  NMR spectrum. The monomer-dimer coalescence in the  $^{13}\text{C}$  and  $^6\text{Li}$  NMR spectra was simulated using WinDNMR<sup>3k</sup> to determine the rate of the dimer to monomer interconversion.

**1-Lithio-5-methylselenophene (3).** To a nitrogen-purged solution of 2-methylselenophene (**16**, 88 mg, 0.608 mmol) in 2.6 mL of THF and 0.6 mL of Me<sub>2</sub>O in a septum-capped 10-mm NMR tube was added 1.1 equiv of *t*-BuLi (0.42 mL of 1.58 M solution).  $^{13}\text{C}$  and  $^{77}\text{Se}$  NMR spectra were taken at  $-130\text{ }^\circ\text{C}$ . Spectra are shown in Figure 4. The sample (originally 0.2 M) was diluted by a factor of 4, and  $^{77}\text{Se}$  spectra were to determine the concentration dependence of the two signals at  $\delta$  715 (monomer) and  $\delta$  729 (dimer).

**Variable Temperature  $^{13}\text{C}$  and  $^6\text{Li}$  NMR Experiment of 4 and Line Shape Simulation of the Dimer Coalescence.** 3-(*N,N*-Dimethylaminomethyl)thiophene (**17**, 93 mg, 0.52 mmol) was added to a dry, N<sub>2</sub>-purged 10 mm NMR tube sealed with a septum. THF (1.8 mL), Et<sub>2</sub>O (1.2 mL), and (Me<sub>3</sub>-Si)<sub>3</sub>CH (3  $\mu\text{L}$ )<sup>3j</sup> were added, and the solution was cooled to  $-78\text{ }^\circ\text{C}$ . *n*-BuLi (2.6 M, 0.21 mL, 0.55 mmol) was added slowly, and the sample was mixed by shaking the NMR tube. A series of  $^{13}\text{C}$  and  $^6\text{Li}$  NMR spectra were acquired between  $-124$  and  $-71\text{ }^\circ\text{C}$ . Spectra and data are reported in Figures 5 and 6 and Tables S-4, S-5 and S-6.<sup>7</sup> Me<sub>2</sub>O (0.7 mL) was added and  $^{13}\text{C}$  and  $^6\text{Li}$  NMR spectra were acquired between  $-142$  and  $-21\text{ }^\circ\text{C}$ . The interconversion of the A-, B- and C-type dimers was simulated using a 3 spin (for  $^{13}\text{C}$ ) or 4 spin (for  $^6\text{Li}$ ) simulation in WinDNMR.<sup>3k</sup>

**Variable Temperature  $^{13}\text{C}$  and  $^6\text{Li}$  NMR Experiment of 5 and Determination of the Rate of Dimer to Monomer Interconversion.** 3-(Methoxymethyl)thiophene (**21**, 89 mg, 0.69 mmol) was added to a dry, N<sub>2</sub>-purged 10-mm NMR tube sealed with a septum. THF (1.0 mL) was added, and the solution was cooled to  $-78\text{ }^\circ\text{C}$ . *n*-BuLi (2.5 M, 0.28 mL, 0.69 mmol) was added slowly, and the sample was mixed by shaking the NMR tube. The sample was stored at  $-78\text{ }^\circ\text{C}$  for 7 days while a powdery precipitate formed. The solvent was removed, THF (0.6 mL) was added, the sample was shaken until the solid dissolved, and Et<sub>2</sub>O (0.4 mL) was added. After 1 day at  $-78\text{ }^\circ\text{C}$  a precipitate formed. The solvent was removed, and the solid was dissolved in THF (1.5 mL). Me<sub>2</sub>O (1.0 mL), Et<sub>2</sub>O (0.5 mL), and (Me<sub>3</sub>Si)<sub>3</sub>CH (2  $\mu\text{L}$ )<sup>3j</sup> were added.  $^{13}\text{C}$  and  $^6\text{Li}$  NMR spectra were acquired between  $-146$  and  $-73\text{ }^\circ\text{C}$ . Spectra and data are reported in Figure 10 and Tables S-7.<sup>7</sup> The  $^{13}\text{C}$  NMR spectra near coalescence of the monomer and dimer were simulated using a 2-spin simulation in

WinDNMR to determine the rate of dimer to monomer interconversion.<sup>3k</sup>

**Acknowledgment.** We thank NSF for financial support (CHE-0074657) and funding for instrumentation (NSF CHE-9709065, CHE-9304546). Brian J. Brandstetter is also acknowledged for his aid in synthesizing some of the 2-thienyllithium precursors. Preliminary experiments of 2-thienyllithium were performed by Wesley L. Whipple.

**Supporting Information Available:** Experimental procedures for the preparation of compounds and NMR samples; <sup>6</sup>Li, <sup>13</sup>C, and <sup>31</sup>P NMR spectra of NMR experiments not presented in the main body of this paper; tables of data for DNMR simulations; X-ray crystal structure data for **5** in CIF format. This material is available free of charge via the Internet at <http://pubs.acs.org>.

JO050592+